**Electronic Supplementary Information**

# Single transition metal atom centered clusters activating semiconductor surface lattice atoms for efficient solar fuel production

Kai Zhang,‡[ab] Chen Sun,‡[a] Tao Chen,‡[c] Fujun Niu,[d] Zhiyi Huang,[a] Qi Gao,[a] Cuiping Xu,[a] Xingjian Zhang,[a] Qixiang Pian,[a] Kunhong Che,[a] Lei Gao,[e] Xianglei Liu,[ab] and Yimin Xuan*[ab]

[a.] College of Energy and Power Engineering, Nanjing University of Aeronautics and Astronautics, Nanjing 210016, China. E-mail: ymxuan@nuaa.edu.cn
[b.] Key Laboratory of Thermal Management and Energy Utilization of Aviation Vehicles, Ministry of Industry and Information Technology, Nanjing 210016, China
[c.] Research Laboratory for Biomedical Optics and Molecular Imaging, CAS Key Laboratory of Health Informatics, Shenzhen Institute of Advanced Technology, Chinese Academy of Sciences, Shenzhen 518055, China
[d.] International Research Center for Renewable Energy, State Key Laboratory of Multiphase Flow in Power Engineering, Xi'an Jiaotong University, Xi'an 710049, China
[e.] Beijing Advanced Innovation Center for Materials Genome Engineering, Institute for Advanced Materials and Technology, University of Science and Technology Beijing, Beijing 100083, China

‡These authors contributed equally to this work.

*e-mail: ymxuan@nuaa.edu.cn

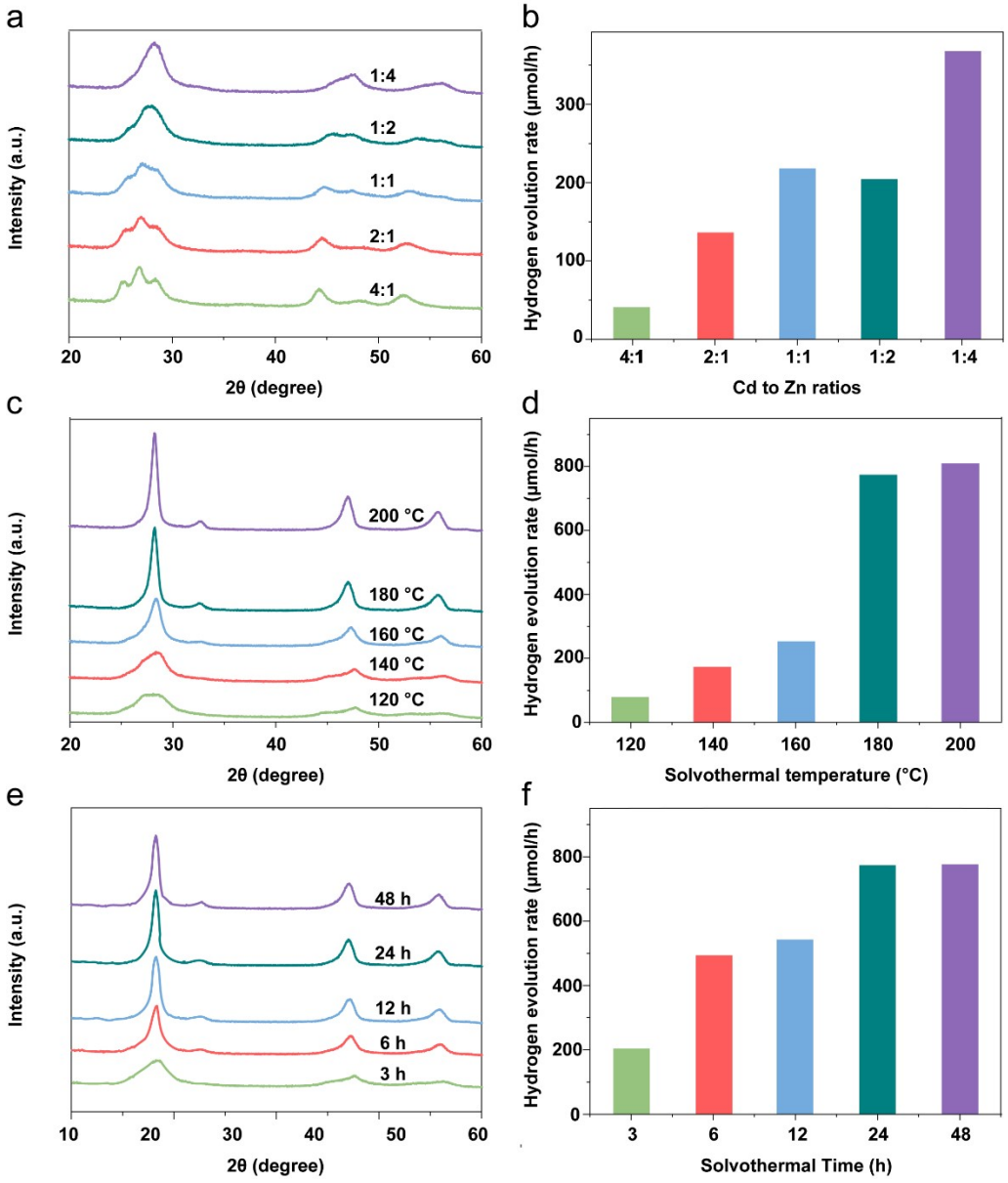


**Fig. S1** Optimization of the synthesis parameters for $Cd_{1-x}Zn_xS$ photocatalysts. XRD patterns and photocatalytic performance of (a-b) $Cd_{1-x}Zn_xS$ photocatalysts with different Cd to Zn ratios, (c-d) $Cd_{0.2}Zn_{0.8}S$ synthesized at different temperatures for 24 h, and (e-f) $Cd_{0.2}Zn_{0.8}S$ synthesized at 180 ℃ for different times.

The synthetic conditions for $Cd_{1-x}Zn_xS$ photocatalysts have been optimized to achieve an excellent photocatalytic performance in $Na_2S/Na_2SO_3$ aqueous solution under visible light irradiation. $Cd_{1-x}Zn_xS$ photocatalyst with a Cd to Zn molar ratio of 1:4 prepared at 180℃ for 24 hours was selected as the prototype photocatalyst, since the further increase of the solvothermal temperature or prolonging of the reaction time can only make a little increase in the photocatalytic activity.

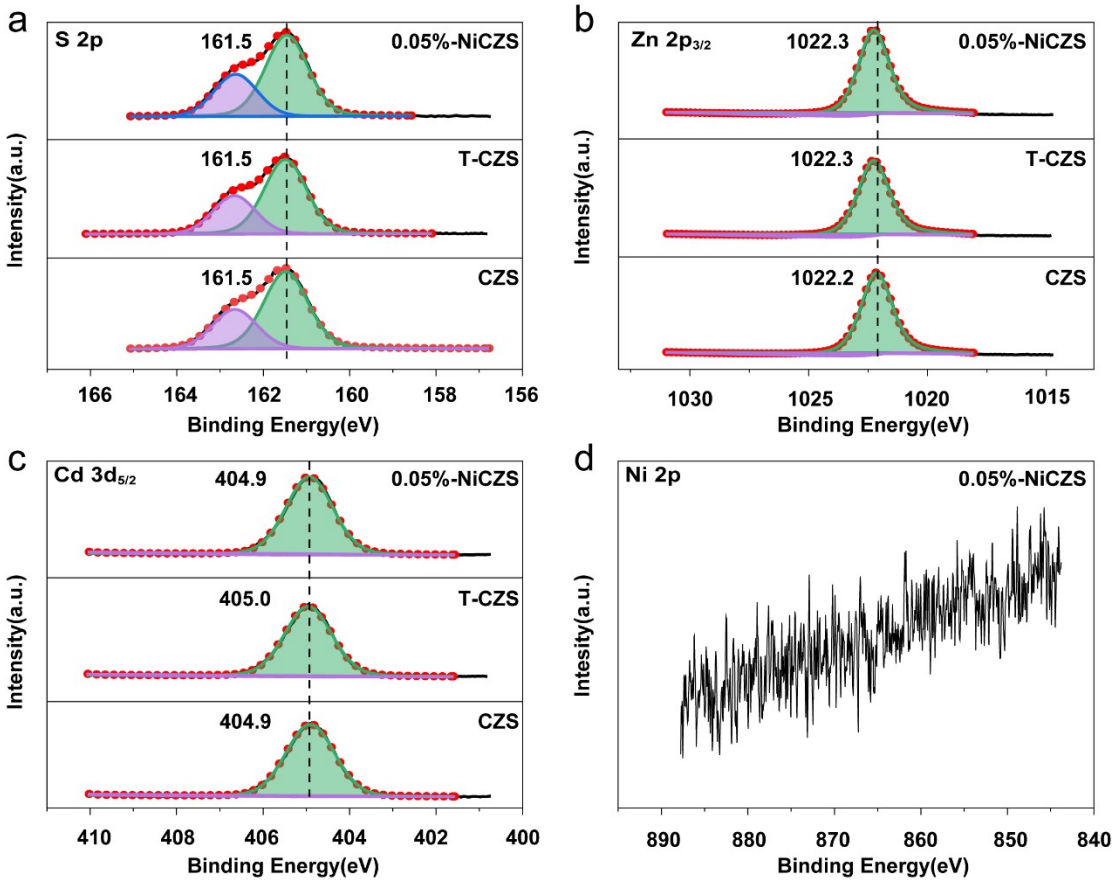


**Fig. S2** S2p, Zn 2p3/2, Cd 3d5/2 and Ni 2p XPS spectra of CZS, T-CZS and 0.05-NiCZS.

There is little difference in the position of XPS peaks among all the three synthesized samples, implying the same chemical states of S, Zn, and Cd elements in these samples. Moreover, according to the Ni 2p spectrum of 0.05-NiCZS in Figure S2d, there is no peaks exist in the binding energy range from 840 to 890 eV. That is, the signals from Ni atoms are too low to be detected by XPS. So, we cannot know the chemical states of Ni atoms from XPS spectra because of the extremely low loading amount.

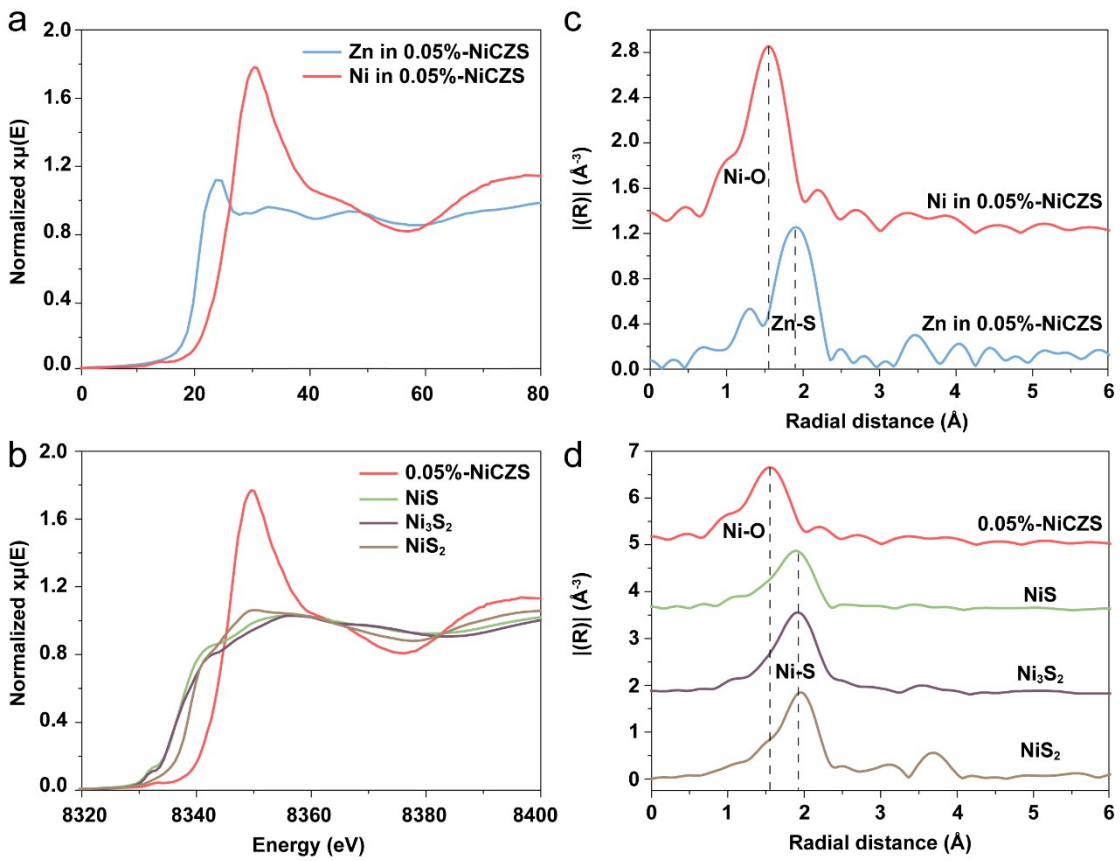


**Fig. S3** XANES profiles and FT-EXAFS signals of of 0.05%-NiCZS as well as reference samples. (a) and (b) Ni and Zn K-edge XANES profiles and FT-EXAFS signals of 0.05%-NiCZS. (c) and (d) Ni K-edge profiles and FT-EXAFS signals of 0.05%-NiCZS, NiS, $Ni_3S_2$, and $NiS_2$.

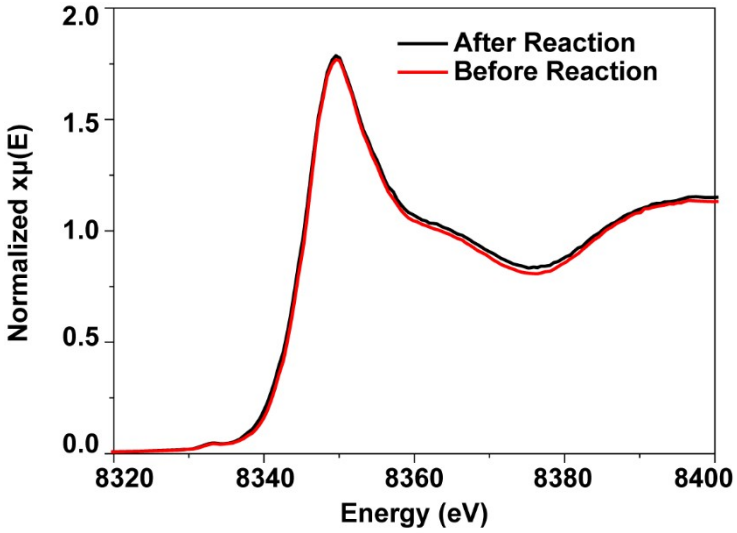


**Fig. S4** Ni K-edge XANES profiles of 0.05%-NiCZS before and after photocatalytic reaction.

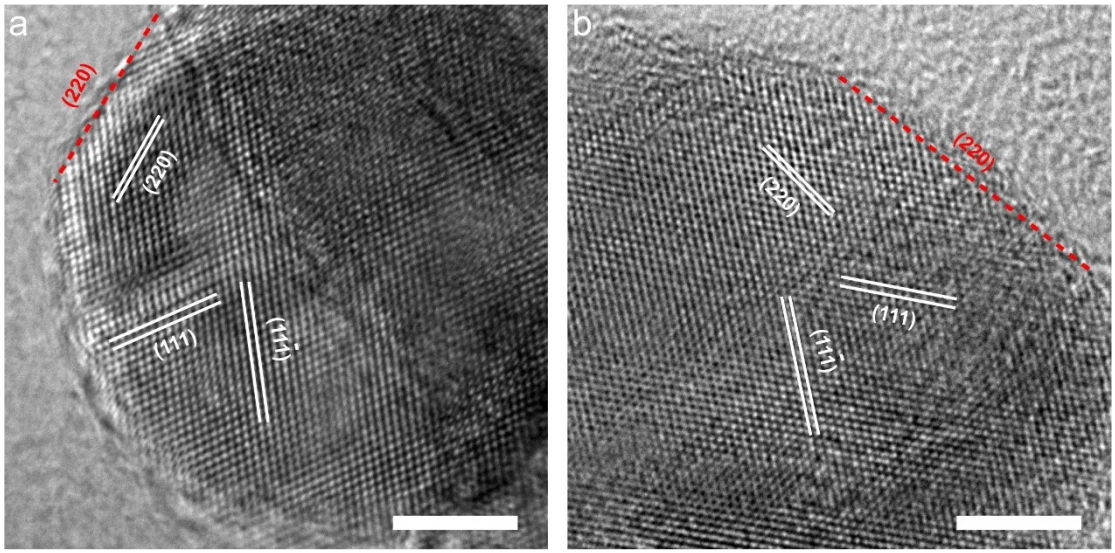


**Fig. S5** High resolution TEM images of (a) CZS and (b) 0.05%-NiCZS. Scale bars: 5 nm.

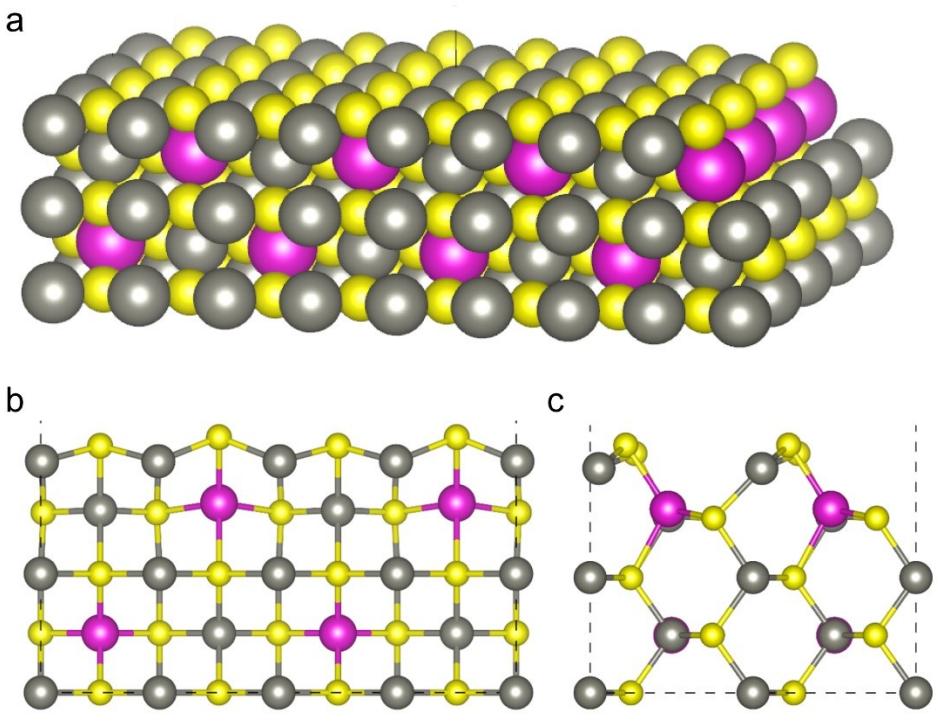


**Fig. S6** Atomic models of CZS (110) surface. (a) Refined atomic structure; (b) Front view; (c) Side view. The gray, purple, and yellow spheres represent Zn, Cd, and S, respectively.

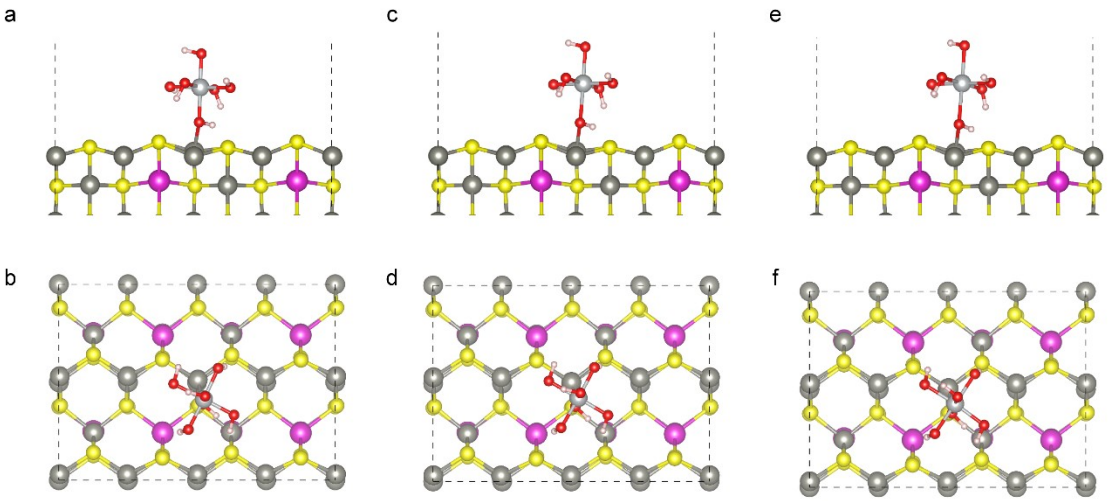


**Fig. S7** Atomic models of CZS (110) surface decorated with different $Ni(O^{Z}H)_6$ clusters via Zn-O-Ni bond linkages. (a) and (b), $Ni(O^{1.33}H)_6$; (c) and (d), $Ni(O^{1.5}H)_6$; (e) and (f), $Ni(O^{1.66}H)_6$.

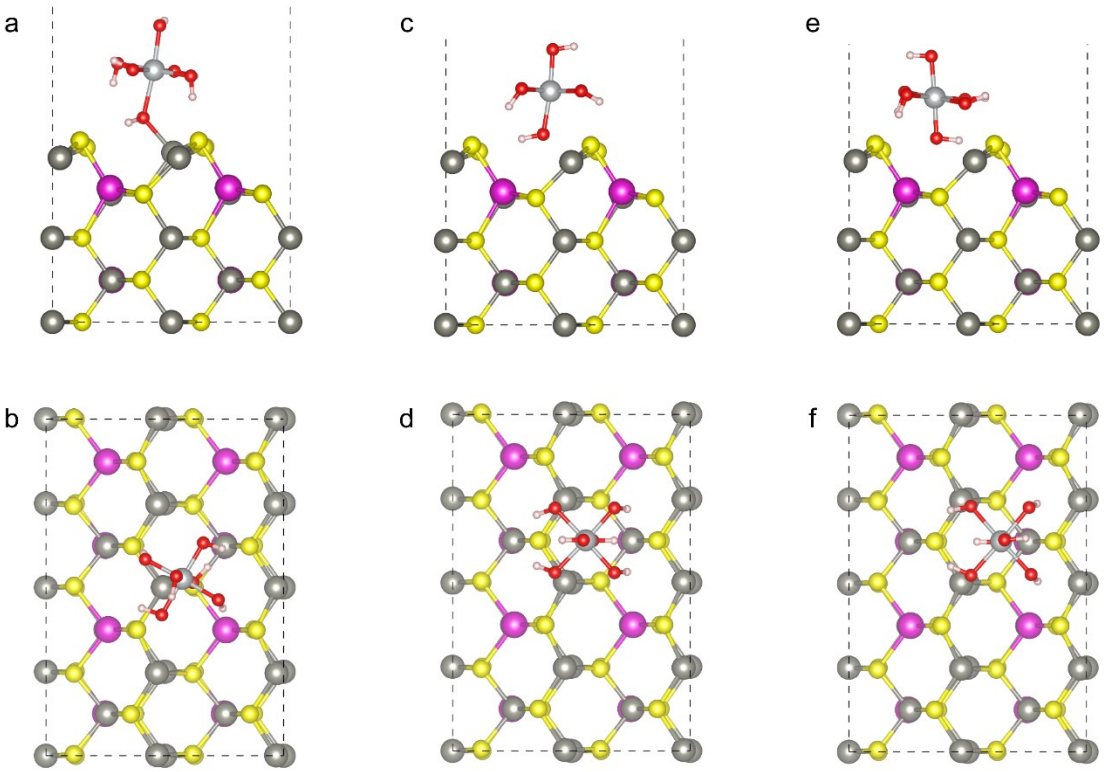


**Fig. S8** Atomic models of CZS (110) surface decorated with $Ni(O^{1.5}H)_6$ clusters at different sites. (a) and (b), atop site; (c) and (d), hollow site; (e) and (f), bridge site.

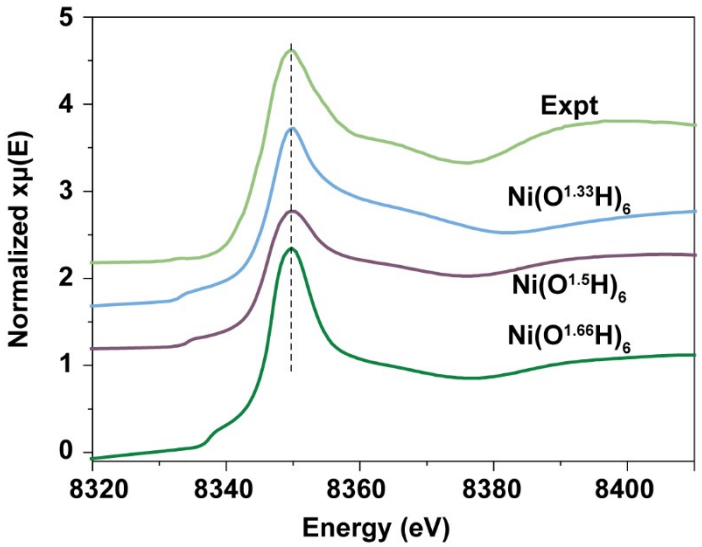


**Fig. S9** Calculated XANES profiles at Ni K-edge of CZS (110) surface with different $Ni(O^ZH)_6$ clusters decorated atop the Zn atom.

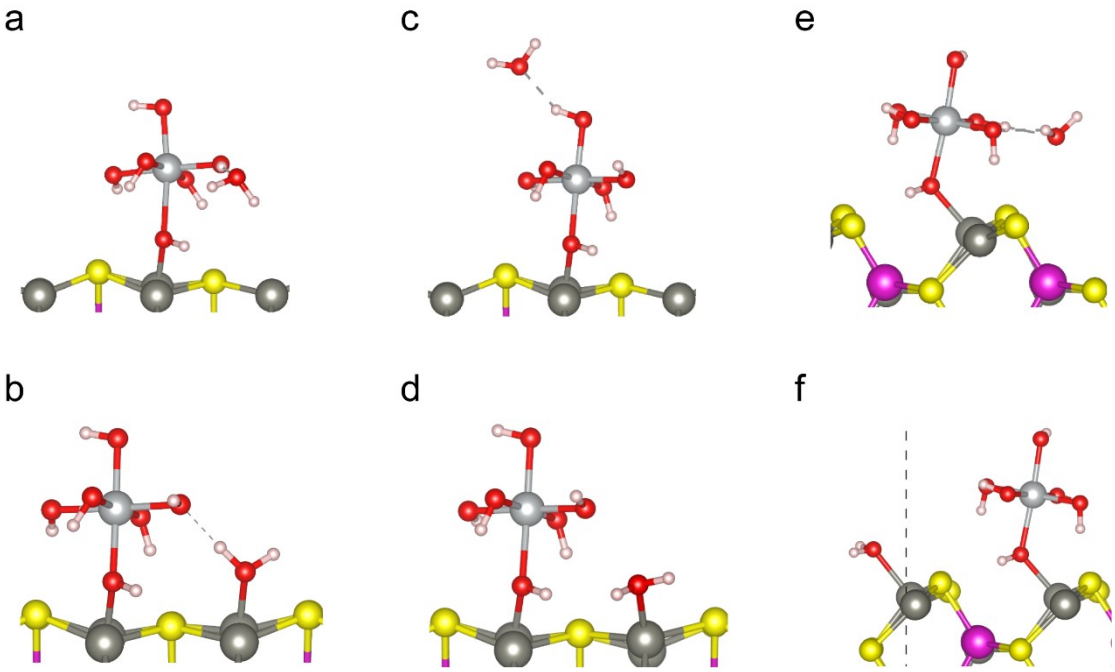


**Fig. S10** Atomic models of $H_2O$ molecule adsorbed at different sites of the $Ni(O^{1.5}H)_6$ cluster decorated CZS (110) surface. (a), (c), and (e) $H_2O$ molecule adsorbed at the sites around $Ni(O^{1.5}H)_6$ cluster; (b), (d), and (f) $H_2O$ molecule adsorbed at different sites on the CZS (110) surface.

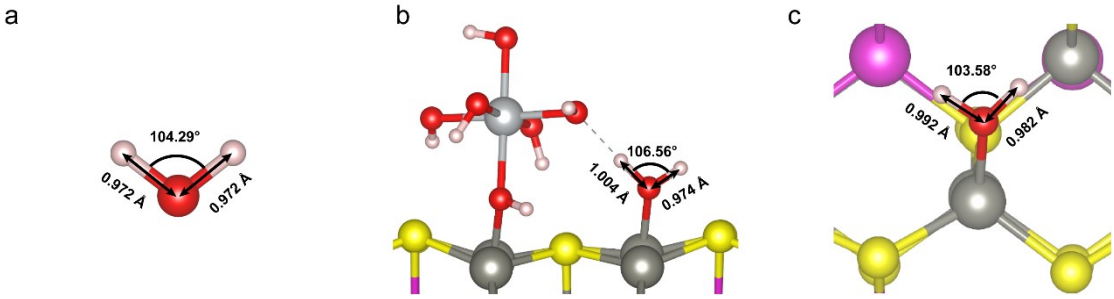


**Fig. S11** Bond angle and bond lengths of $H_2O$ molecule before and after adsorption. (a) Free $H_2O$ molecule; (b) $H_2O$ molecule adsorbed on the Zn atom besides the $Ni(O^{1.5}H)_6$ cluster; (c) $H_2O$ molecule adsorbed on CZS (110) surface.

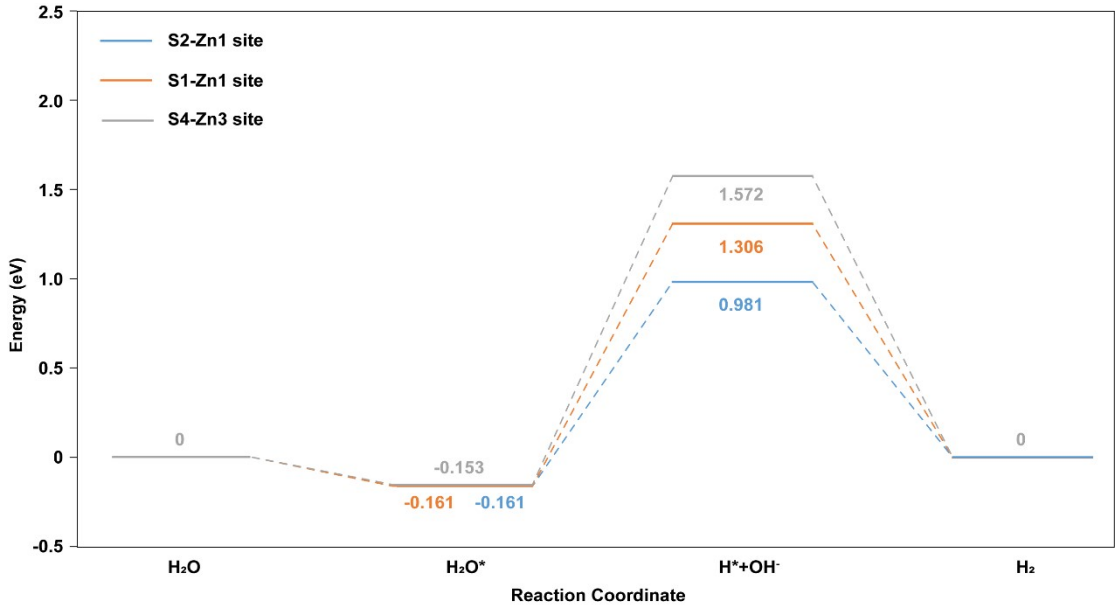


**Fig. S12** Free energy diagram for HER over different sites of the $Ni(O^{1.5}H)_6$ cluster decorated CZS (110) surface.

The kinetic energy barriers of the water dissociation step at different sites of the CZS surface decorated with $Ni(O^{1.5}H)_6$ cluster are also calculated, all of which are much less than that on the pristine CZS surface (1.850 eV).

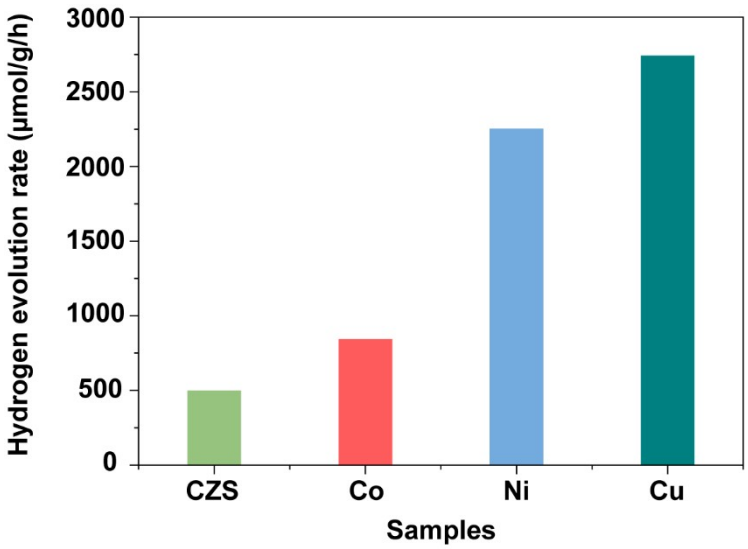


**Fig. S13** Photocatalytic performance of CZS decorated with different transition metal compounds. The weight ratios of transition metals to CZS are all 1.0 wt%.

Co and Cu compounds were also decorated onto the surface of $Cd_{0.2}Zn_{0.8}S$ photocatalyst via the same low concentration metal salt solution solvothermal strategy. The samples decorated 1.0 wt% of Co, Ni and Cu were all employed in photocatalytic $CO_2$ reduction. All the samples show excellent activity for hydrogen production in $NaHCO_3/Na_2SO_3$ solution under $CO_2$ atmosphere, while little or no CO and $CH_4$ can be found in the gaseous products. That is, the low concentration metal salt solution solvothermal strategy is a generalized method to activate semiconductor surface for photocatalytic reaction. But it is more effective for hydrogen production other than $CO_2$ reduction at the present stage.

**Table S1** Summary of photocatalytic hydrogen evolution activities of Zn-rich $Cd_xZn_{1-x}S$ in literatures.

| Photocatalyst | Cocatalyst | Amount | Light Source | Sacrificial Reagent | Activity | Increment | AQY | REF |
|---|---|---|---|---|---|---|---|---|
| $Cd_{0.2}Zn_{0.8}S$ | Ni clusters | 0.05 wt% | 300 W Xe lamp<br>λ≥420 nm | 0.35 M $Na_2S$<br>0.25 M $Na_2SO_3$ | 6475<br>umol $g^{-1}$ $h^{-1}$ | 68% | 15.8%@425 nm | This Work |
| $Cd_{0.3}Zn_{0.7}S$ | $Ni(OH)_2$ | 10 wt% | 300 W Xe lamp<br>λ≥420 nm | 0.35 M $Na_2S$<br>0.25 M $Na_2SO_3$ | 58900<br>umol $g^{-1}$ $h^{-1}$ | 102% | | 1 |
| $Zn_{0.8}Cd_{0.2}S$ | $Ni(OH)_2$ | 0.6 mol% | 300 W Xe lamp<br>λ≥420 nm | 20 vol%<br>TEOA | 7160<br>umol $g^{-1}$ $h^{-1}$ | 2448% | 29.5%@420 nm | 2 |
| $Cd_{0.1}Zn_{0.9}S$ | $Ni^{2+}$ | 0.1 wt% | 350 W Xe lamp<br>λ≥420 nm | 0.35 M $Na_2S$<br>0.25 M $Na_2SO_3$ | 191.01<br>umol $g^{-1}$ $h^{-1}$ | 60% | 6.77%@420 nm | 3 |
| $Cd_{0.1}Zn_{0.9}S$ | $Ni^{2+}$ | 0.7 wt% | 350 W Xe lamp<br>λ≥420 nm | 0.35 M $Na_2S$<br>0.25 M $Na_2SO_3$ | 403.75<br>umol $g^{-1}$ $h^{-1}$ | 300% | 14.36% @420nm | 4 |
| $Cd_{0.25}Zn_{0.75}S$ | $Ni^{2+}$ | 0.1 wt% | 380 nm LED | 0.117 M $Na_2S$<br>0.16 M $Na_2SO_3$ | 109800<br>umol $g^{-1}$ $h^{-1}$ | 130% | 14.9%@380 nm | 5 |
| $Zn_{0.8}Cd_{0.2}S$ | $Ni^{2+}$ | 5 wt% | 300 W Xe lamp<br>λ≥420 nm | 0.35 M $Na_2S$<br>0.25 M $Na_2SO_3$ | 33810<br>umol $g^{-1}$ $h^{-1}$ | 366% | | 6 |
| $Zn_{0.65}Cd_{0.35}S$ | CuS | 5.9 mol% | 300 W Xe lamp<br>λ≥420 nm | 0.1 M $Na_2S$<br>0.1 M $Na_2SO_3$ | 1833<br>umol $g^{-1}$ $h^{-1}$ | 1796% | 8.1%@420 nm | 7 |

**Table S2** Ni to CZS wight ratios of *x*-NiCZS obtained from ICP-AES analysis.

| | Ni to CZS weight ratio (%) | | | |
|---|---|---|---|---|
| Nominal value | 0.01 | 0.05 | 0.10 | 0.20 |
| Practical value | 0.016 | 0.036 | 0.047 | 0.077 |

**Table S3** Ni K-edge EXAFS curve fitting parameters.[a]

| Sample | Path | N | R (Å) | σ2 (Å2) | $\Delta E_0$ (eV) | R% |
|---|---|---|---|---|---|---|
| Ni foil[b] | Ni-Ni | 12* | 2.48±0.00 | 6.5±0.2 | 7.1±0.4 | 0.002 |
| NiO[c] | Ni-O | 6.6±0.5 | 2.08±0.01 | 6.3±0.8 | -6.0±2.0 | 0.008 |
| | Ni-Ni | 12.3±0.4 | 2.95±0.00 | 5.6±0.5 | -6.7±0.8 | |
| 0.05-NiCZS[d] | Ni-O | 6.3±0.4 | 2.04±0.00 | 4.3±1.1 | -5.4±1.5 | 0.008 |

[a] N, coordination number; R, distance between absorber and backscatter atoms; $\sigma^2$, Debye-Waller factor to account for both thermal and structural disorders; $\Delta E_0$, inner potential correction; R factor (%) indicates the goodness of the fit. S0 was fixed to 0.85 as determined from Ni foil fitting. * indicate fixed coordination number (N) according to the crystal structure. [b] Fitting range: $3 \leq k$ (/Å) $\leq 12.5$ and $1 \leq R$ (Å) $\leq 3$. [c] Fitting range: $3 \leq k$ (/Å) $\leq 14$ and $1 \leq R$ (Å) $\leq 3.1$. [d] Fitting range: $3 \leq k$ (/Å) $\leq 15$ and $1 \leq R$ (Å) $\leq 2.1$.

**Table S4** Ni-O bond lengths of the different $Ni(O^ZH)_6$ clusters adsorbed on CZS (110) surface.

| Terminating Atom | Bond lengths (Å) | | | | | | |
|---|---|---|---|---|---|---|---|
| | Ni-O1 | Ni-O2 | Ni-O3 | Ni-O4 | Ni-O5 | Ni-O6 | Zn-O5 |
| $^{1.33}H$ | 1.89 | 1.87 | 1.89 | 1.88 | 1.94 | 1.85 | 2.12 |
| $^{1.5}H$ | 1.91 | 1.88 | 1.92 | 1.89 | 2.22 | 2.04 | 2.1 |
| $^{1.66}H$ | 1.99 | 1.98 | 2.02 | 1.98 | 2.32 | 2.11 | 2.1 |

**Table S5** Absorption energy of $H_2O$ at different sites of CZS decorated with $Ni(O^{1.5}H)_6$ cluster.

| Adsorption sites | $NiO_6$ Cluster | | | CZS surface | | |
|---|---|---|---|---|---|---|
| | Site 1 | Site 2 | Site 3 | Zn1 | Zn3 | Zn4 |
| Adsorption energy (eV) | 0.308 | 0.232 | 0.295 | -0.161 | -0.153 | -0.134 |

Reference

1. B. Lv, X. Feng, X. Xi, X. Feng, Z. Yuan, Y. Yang and F. Zhang, *J. Colloid Interface Sci.*, 2021, **601**, 177-185.

2. J. Ran, J. Zhang, J. Yu and S. Z. Qiao, *ChemSusChem*, 2014, **7**, 3426-3434.

3. X. H. Zhang, D. W. Jing, M. C. Liu and L. J. Guo, *Catal. Commun.*, 2008, **9**, 1720-1724.

4. X. H. Zhang, D. W. Jing and L. J. Guo, *Int. J. Hydrogen Energy*, 2010, **35**, 7051-7057.

5. M. A. Mersel, L. Fodor, P. Pekker, E. Mako and O. Horvath, *Molecules*, 2022, **27**.

6. Y. Luo, X. Zhang, C. Huang, X. Han, Q. Jiang, T. Zhou, H. Yang and J. Hu, *ACS Omega*, 2021, **6**, 13544-13553.

7. W. Zhang and R. Xu, *Int. J. Hydrogen Energy*, 2009, **34**, 8495-8503.